Scilight

Sustainable Engineering Novit
https://www.sciltp.com/journals/sen

Review

Metal–Organic Frameworks: Morphological Diversity and Applications of Rod, Sheet, Cubic and Octahedral Structures

Surulivel Gokul Eswaran [1,2], Yajun Gao [1,*] and Aijian Wang [3]

[1] School of Food Science and Technology, Yangzhou University, Yangzhou 225127, China
[2] School of Chemistry and Chemical Engineering, Yangzhou University, Yangzhou 225127, China
[3] School of Chemistry & Chemical Engineering, Jiangsu University, Zhenjiang 212013, China
* Correspondence: gaoyajun@yzu.edu.cn

How To Cite: Eswaran, S.G.; Gao, Y.; Wang, A. Metal–Organic Frameworks: Morphological Diversity and Applications of Rod, Sheet, Cubic and Octahedral Structures. *Sustainable Engineering Novit* **2026**, *2*(1), 5. https://doi.org/10.53941/sen.2026.100005

Received: 30 January 2026
Revised: 14 March 2026
Accepted: 18 March 2026
Published: 27 March 2026

Abstract: Metal–Organic Frameworks (MOFs) have emerged as versatile crystalline materials morphology significantly governs their physicochemical properties. The novelty of morphological diversity in MOFs is particularly evident in their 1D, 2D and 3D frameworks, each offering unique structural advantages and functional opportunities. Each morphology is explored in terms of its structural functionality, synthetic strategies and application potential. The rod-like morphologies for directional transport and anisotropic growth. The sheet-like forms for their ultrathin, high-surface-area characteristics. Cubic frameworks are highlighted for their uniform porosity and stability. Similarly, octahedral structures for their enhanced surface exposure and synthesis pathways are discussed, emphasizing morphology control through ligand design, solvent modulation and templating approaches. It reveals the shape-dependent properties determine performance. In this study, introduces a comparative perspective on morphology-driven advantages, bridging fundamental insights with practical device engineering. The MOFs based different morphology was used in several applications. The MOFs morphology as a primary parameter, it positions morphology as a central design principle for next-generation MOF-based devices. In future point of view, the MOFs synthesis and their properties were unique and applied in various applications. This comprehensive framework establishes morphology as a key axis for innovation in MOFs research. It paves the way for tailored applications in energy, environment and materials science.

Keywords: MOFs; morphology; rod; sheet; cubic; octahedral

1. Introduction

In recent years, porous materials have attracted significant interest due to their exceptional structural and functional properties [1]. The continuous development of new classes of porous solids has broadened the scope of materials science. Recent times, there are several porous materials have established such as zeolites, metal–organic frameworks, periodic mesoporous organosilicas, hyper-crosslinked polymers, polymers of intrinsic microporosity, conjugated microporous polymers, porous aromatic frameworks and covalent organic frameworks [2–5]. Among these, metal–organic frameworks (MOFs) is a unique material because of their exceptionally high surface area, tunable porosity and remarkable thermal stability [6,7]. The ability to exhibit diverse functionalities such as photocatalytic activity, electronic conductivity, magnetic behavior and even biological interactions [8–10]. The Nobel Prize in chemistry was awarded to Omar M. Yaghi, Susumu Kitagawa and Richard Robson for their pioneering contributions to the design and synthesis of metal organic frameworks in 2025 [11,12]. Yaghi's rational approach to constructing strong MOFs [13]. Kitagawa's demonstration of their flexibility and gas transport

properties [14]. Robson's creation of spacious, well-ordered architecture collectively established the foundation for tailoring porous materials with vast internal surface areas and customizable chemical environments [15]. These breakthroughs have attracted MOFs as a further focus in materials research. MOFs have structurally composed of metal centers coordinated with organic linkers. The numerous frameworks based on transition metals and alkaline-earth metals have been reported, each offering unique structural features [16]. Their applications in gas storage, molecular separation, catalysis, sensing, ion exchange, drug delivery and adsorption technologies [17,18].

The morphological diversity of MOFs, ranging from 0D to 3D structures, plays a crucial role in determining their properties and potential applications [19]. Facets that grow more slowly are expressed on the crystal surface. It controls these growth dynamics and allows to tune external surface area and catalytic activity by exposing specific active sites. Interestingly, 0D MOFs synthesized as nanoparticles or quantum dot-like structures, exhibit high surface area and tunable porosity [20]. 1D MOFs, typically rod-like or wire-shaped are formed through controlled growth along a single axis and display anisotropic properties that enhance ion transport and photocatalytic activity [21]. 2D MOFs produced as ultrathin nanosheets or layered frameworks, provide exceptionally large surface areas and fast diffusion pathways [22]. Finally, 3D MOFs such as cubic or octahedral frameworks are highly crystalline and interconnected, offering strong mechanical stability and versatile pore systems [23,24]. The ability to tailor MOF morphology through synthetic innovations not only enriches their structural diversity but also expands their integration into advanced applications (Figure 1).

Dimension	Description	Synthetic Approaches	Properties	Applications
0D (Zero-Dimensional)	Nanoparticles or quantum dot-like MOFs with confined structures	Controlled nucleation, surfactant-assisted synthesis	High surface area, discrete particle size, tunable porosity	Catalysis, drug delivery, sensing
1D (Rod-like/Linear)	Nanorods, wires or chain-like MOFs with growth along one axis	In-Situ Electrochemical, Hydrothermal method, Solvothermal method, Microwave-assisted method and Sonication method	Enhanced ion/electron transport, anisotropic properties	Supercapacitor, CO_2 adsorption, Catalyst, Photodegradation and Sensor Applications
2D (Sheet-like)	Ultrathin nanosheets or layered MOFs	Surfactant-assisted, Solvothermal method, Regulator-assisted method, Template-assisted method and Interface synthesis method	Large surface area, high aspect ratio, fast diffusion pathways	Sensor, Supercapacitor, Catalysis, Electrocatalytic and Photocatalytic hydrogen production applications
3D (Cubic/Octahedral frameworks)	Highly crystalline, interconnected porous networks	Microwave-assisted method, Solvothermal method, Pulsed laser ablation method, Electrochemical method, Sonication method	Strong mechanical stability, interconnected pore systems	Catalysts for hydrogen evolution reaction, Photocatalysis, Lithium-Ion batteries, Sensor, CO_2 reduction and Electrochemical capacitor applications

Figure 1. Comparison of the different morphologies of MOFs (0D, 1D, 2D and 3D) along with their respective applications.

A wide range of synthetic methods have been developed to produce MOFs including solvothermal and hydrothermal methods, vapor deposition, microwave synthesis, sonochemical approaches, electrochemical methods and interfacial synthesis [25–27]. These techniques help to control parameters such as reactant concentration, reaction temperature and time to regulate crystal growth and morphology. The application of MOFs with different morphologies remains an evolving field. While 1D rods, 2D sheets and 3D cubic or octahedral structures each offer unique advantages, challenges persist in achieving precise control over size, shape and stability. Future research will likely focus on integrating advanced synthesis techniques, computational modeling and hybrid material design. In this review, we have explored the different morphology of MOFs (rod, sheet, cubic and octahedral) synthesis methods and their applications. Finally, we have discussed the MOFs and their morphology from a future point of view.

2. Synthesis of MOFs with Different Morphology

2.1. Synthesis of Rod-Like MOFs Structures

2.1.1. *In-Situ* Electrochemical Synthesis Method

Chen et al., investigated the *in situ* electrochemical synthesis of rod like Ni-MOFs to establish a controllable and efficient method for MOFs fabrication (Figure 2a) [28]. In this approach, nickel foam (NF) served as both the substrate and the source of Ni^{2+} ions. The direct growth of Ni-MOFs arrays on its surface. The products required no post treatment and could be immediately employed as binder free electrode materials, thereby enhancing electron and ion transport at the electrode interface. Trimesic acid as a starting material dissolved in ethanol and NH_4F was dissolved in deionized water. The electrolyte was gradually added into solution, this solution under stirring at room temperature. During electrosynthesis, the NF acted as the anode and a platinum mesh as the cathode with deposition carried out at a certain voltage in a water bath. The influence of reaction duration, syntheses were performed for 0.5, 1.0 and 1.5 h and the samples were designated Ni-MOF 0.5 h, Ni-MOF 1 h and Ni-MOF 1.5 h, respectively. This *in-situ* electrochemical strategy not only simplifies the synthesis process but also produces structurally unique Ni-MOFs with promising applications in energy storage and conversion.

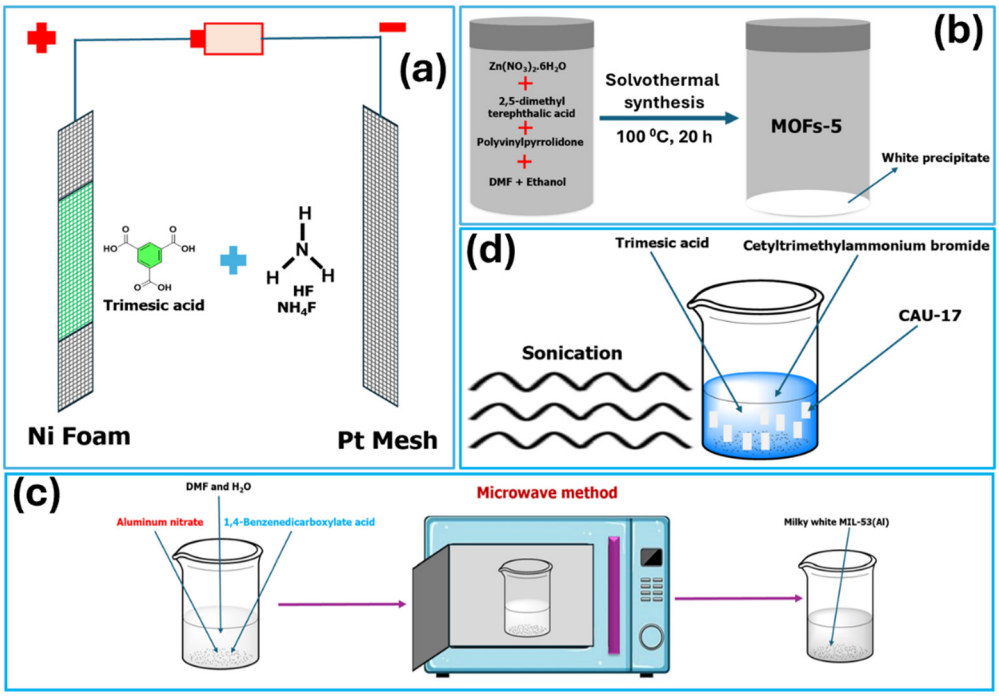

Figure 2. (**a**) The schematic diagram of the *in-situ* electrochemical synthesis of Ni-MOFs. (**b**) Solvothermal synthesis of MOFs-5. (**c**) Microwave assisted method of MIL-53(Al). (**d**) Sonication method of CAU-17.

2.1.2. Hydrothermal Method

Liu and their group members reported the successful synthesis of MOFs derived Fe_7S_8/C rod-like composites by using hydrothermal method [29]. The study focused on the synergistic interaction between Fe_7S_8 and carbon. The relative proportions of these two components are controlled by adjusting the dosage of ferric salt. It influence on the electromagnetic parameters and absorption efficiency. The nanosheet-assembled architecture was obtained through pyrolysis of the organic framework and the formation of Fe_7S_8, which produced a rough surface. During high-temperature sulfuration, a small fraction of iron was reduced to metallic Fe. The presence of C–O, C=O and C–C species confirmed abundant functional groups in the amorphous carbon. It serves as polarization centers that enhance electromagnetic absorption. The importance of tuning the Fe_7S_8/carbon ratio to maximize absorption properties. The composites was optimized by impedance matching and strong energy dissipation in outstanding absorption behavior.

2.1.3. Solvothermal Method

Wang and their colleagues reported the synthesis of rod-like MOFs (MOF-5) materials through a solvothermal approach (Figure 2b) [30]. Initially, Zinc nitrate hexahydrate, 2,5-dimethylterephthalic acid and polyvinylpyrrolidone

were dissolved in a solvent mixture of dimethylformamide (DMF) and ethanol to form a homogeneous solution. This mixture was transferred into a Teflon-lined stainless-steel autoclave and maintained at 100 °C for 20 h. After cooling, the white precipitate was separated by centrifugation, thoroughly washed with DMF and chloroform and dried at 120 °C in a tray dryer. The process yielded uniform rod-like MOF-5 nanomaterials formed. The O–H stretching vibration was observed in water molecules adsorbed at Zn sites with hydrogen also engaged in hydrogen bonding to displaced oxygen on the linker. In addition, the Zn–O stretching mode within the tetrahedrally coordinated Zn_4O cluster. These results confirmed that the phonon vibration modes of the synthesized material matched those of standard MOF-5, verifying the successful formation of MOF-5 nanostructures.

2.1.4. Microwave-Assisted Method

Tang et al., reported the microwave-assisted solvothermal synthesis of rod-like aluminum terephthalate [MIL-53(Al)] [31]. Some aluminum-based MOFs known for its high porosity and structural stability (Figure 2c). The MIL-53(Al) was prepared using water and DMF as co-solvents under microwave irradiation. The synthesis parameters systematically varied to evaluate their influence on crystal structure, morphology and adsorption performance. Key factors including pre-mixing conditions, microwave temperature, applied power and reaction time were adjusted to optimize the material. The sample prepared under stirring conditions at 130 °C, 200 W and 3 h exhibited high crystallinity and a distinct rod-like morphology. The microwave-assisted approach significantly shortened reaction time while producing well-defined structures. The synthesis parameters directly impacts the structural and functional properties of the material.

2.1.5. Sonication Method

Wang and co-workers prepared a sustainable strategy for synthesizing stable MOFs with permanent, highly ordered porosity under ambient conditions [32]. It eliminates the need for toxic solvents or prolonged high-temperature reactions. Their work focused on the rapid and eco-friendly preparation of bismuth-based MOFs (Bi-MOFs), specifically $[Bi_9(C_9H_3O_6)_9(H_2O)_9]$, known as CAU-17 using a surfactant-mediated sonochemical approach in water (Figure 2d). This method employed cetyltrimethylammonium bromide (CTAB) amphiphilic molecules as structure-directing agents to regulate dehydration of non-coordinated water and enhance ligand deprotonation, thereby facilitating controlled coordination and crystallization in aqueous media. The CAU-17 exhibited remarkable functional properties including efficient iodine capture. It enabled by its broad pH tolerance and phosphate-responsive degradation in intestinal environments. One of the challenges in rod shape MOFs synthesis is the simultaneous formation of multiple crystalline phases, complicating purification. The small amounts of CTAB in methanol promoted pure-phase crystallization of CAU-17, while higher concentrations acted as capping agents to suppress radial growth. Importantly, the optimized sonochemical conditions allowed rapid synthesis of uniform rod-shaped CAU-17 nanocrystals in water without organic solvents. Summary of the rod-shaped MOFs with previously published work revealed in Table 1.

Table 1. Summary of the rod-shaped MOFs with previously published work.

Materials Name	Ligand	Synthesis Method	Solvent	Temperature/ Time	Applications	Ref
Ni-MOFs	Trimesic acid	*In-situ* electrosynthesis method	Ethanol and DMF	70 °C/1.5 h	Supercapacitor	[28]
MOF-derived Fe_7S_8/C	Fumaric acid	Hydrothermal method	Deionized water	100 °C/12 h	Electromagnetic wave absorption	[29]
CTH-16	Benzene-1,2,4,5-tetracarboxylic acid	Solvothermal method	DMF/H_2O/glacial acetic acid	120 °C/72 h	-	[33]
Rod-MOF (Rod-6)	1,3,6,8-tetrakis (p-benzoic acid)pyrene	Solvothermal method	DMF/H_2O	120 °C/72 h	CO_2 adsorption	[34]
ZrBTE rod	4,4′,4″-(benzene-1,3,5-triyl-tris(ethyne 2,1-diyl))tribenzoic acid	Solvothermal method	DMF/acetic acid	-	-	[35]
MOF-5	2,5-dimethylterephthalic acid	Solvothermal method	DMF and ethanol	100 °C/20 h	Removal of U(VI)	[30]
ROD-8	1,3,6,8-tetrakis(p-benzoic acid)pyrene	Solvothermal method	DMF–dioxane H_2O	120 °C/72 h	Gas adsorption	[36]
MIL-53(Al)	1,4-Benzenedicarboxylate acid	Solvothermal method	DMF and H_2O	110 °C/12 h	CO_2 adsorption	[31]
Bi-MOFs	Trimesic acid	Sonication method	MeOH	-	-	[32]
Fe-based MOF@CuO NC	1,3,5-benzenetricarbocylic acid	Co-precipitation method	Deionized water	150 °C/1 h	Catalyst	[37]
Fe–Al BDC	Terephthalic acid	Solvothermal method	DMF	~200 °C/70 h	Photo-degradation	[38]
ROD-95	2,2′-dinitro-4,4′-biphenyldicarboxylic acid	Solvothermal method	DMF	120 °C/72 h	Sensing application	[39]

2.2. Synthesis of Sheet-Like MOFs Structures

2.2.1. Surfactant-Assisted Method

Zhang and his co-workers developed ultrathin MOFs nanosheets through a surfactant-assisted synthesis strategy (Figure 3a) [40]. Surfactants are widely recognized for their ability to regulate nanocrystal growth by selectively binding to specific crystal facets, thereby influencing particle size and morphology. They have also been employed in the fabrication of MOFs metal nanoparticle composites. The polyvinylpyrrolidone (PVP) was introduced as a surfactant during the preparation of Zn-TCPP, it controlled anisotropic crystal growth. The selective attachment of PVP molecules to MOF surfaces guided the formation of nanosheets rather than bulk crystals. It is typically obtained through conventional synthesis without surfactants. The two-dimensional MOFs nanosheets based on tetrakis(4-carboxyphenyl)porphyrin (TCPP) ligands and different metals (Zn, Cu, Cd and Co) were successfully prepared. The surfactant-assisted method proved to be a simple yet versatile method for tailoring MOFs morphology at the nanoscale.

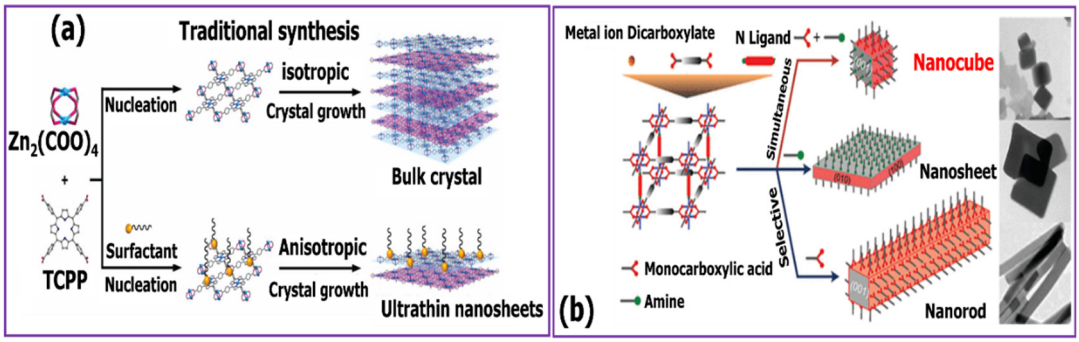

Figure 3. (**a**) The surfactant-assisted synthesis of sheet shape MOFs. Reproduced with permission [40]. Copyright 2015, John Wiley and Sons. (**b**) The synthesis of the materials with different morphologies by using Regulator-assisted synthesis. Reproduced with permission [41]. Copyright 2012, American Chemical Society.

2.2.2. Solvothermal Method

Solvothermal synthesis method is one of the most widely used approaches for fabricating MOFs nanosheets. In this method, metal precursors and organic ligands are dissolved in a solvent, mixed thoroughly and reacted under controlled conditions [42]. The outcome of nanosheet formation is strongly influenced by several parameters including solvent type, reaction temperature, precursor ratios and synthesis duration [43]. Dong et al. demonstrated the preparation of nanostructured conductive MOFs using a solvothermal template strategy. The transformation of insulating MOFs into conductive 2D frameworks (c-MOFs) with tailored morphologies and dimensions [44]. Conventional solvothermal synthesis often yields bulk crystals with needle-like morphologies due to the imbalance between strong in-plane coordination and weak out-of-plane π-stacking. Other approaches such as surface-assisted or interface-mediated synthesis have produced crystalline films. However, achieving a combination of high porosity, efficient mass transport, accessible active sites and intrinsic conductivity in 2D c-MOFs. Their inherent microporosity and dense layer stacking frequently hinder diffusion and limit performance in energy and electronic applications. The solvothermal method families of 2D c-MOFs with diverse chemical compositions, shell structures, dimensions and substrates have been synthesized.

2.2.3. Regulator-Assisted Method

A regulator-assisted synthetic approach offers a promising method to obtain sheet-like MOFs with controlled morphology and enhanced structural uniformity [45]. In this method, small molecular regulators are introduced into the reaction medium to modulate the coordination kinetics between metal ions and organic linkers. Selectively binding or competing with active sites during nucleation, the regulators slow down isotropic crystal growth and favor anisotropic extension, leading to ultrathin sheet-like architectures. The MOFs exhibit large, exposed surface areas, shortened ion diffusion and abundant accessible active centers. This method also provides flexibility, as the type and concentration of regulators can be tuned to adjust thickness, lateral dimensions and crystallinity of the sheets. Its precise control over the final material properties without sacrificing stability or porosity.

Zhu et al. demonstrated this concept by employing dopamine hydrochloride (DA-HCl) as a regulator in the synthesis of Cu-TCPP [TCPP = 4,4,4,4-(porphine-5,10,15,20-tetrayl)tetrakis(benzoic acid))] nanosheets [46]. In their approach, hydrochloric acid facilitated the incorporation of the metal source into the porphyrin ring, while dopamine

acted as an intercalating agent to suppress interlayer stacking. The carboxylate groups of TCPP, dopamine directed the framework to grow preferentially in-plane, yielding ultrathin Cu-TCPP nanosheets. Similarly, Do and their coworkers investigated the use of various amines as regulators to modulate the crystal size and morphology of copper-based MOFs (Figure 3b) [41]. Their findings highlight the versatility of regulator-assisted synthesis in tailoring MOF structures. It offers a practical method to achieve nanosheets and other morphologies with enhanced functional properties.

2.2.4. Template-Assisted Method

Template-assisted synthesis provides a versatile method to engineer sheet-like MOFs with controlled dimensions and uniform morphology. In this approach, soft or hard templates such as layered clays, surfactant assemblies or pre-formed nanosheets are introduced into the reaction system to guide anisotropic crystal growth [47]. The template acts as a structural scaffold, restricting nucleation in certain directions and promoting lateral expansion. The ultrathin MOFs sheets with high aspect ratios. The template type, concentration and removal strategy are more important. The thickness and lateral size of the MOFs sheets can be precisely adjusted. After synthesis, the template can be removed through mild chemical etching or thermal treatment. After that, the leaving behind free-standing MOFs nanosheets with abundant exposed active sites and enhanced accessibility. These sheet-like MOFs combine large surface area with short diffusion pathways. Its rapid ion transport and efficient electron transfer.

For instance, Dong and co-workers reported the preparation of ZIF-67 nanosheets using a salt-templated confinement strategy [48]. In their method, a large amount of NaCl was employed to generate microcrystal planes. It restricts the extension of MOFs precursors along the plane and preventing the formation of bulk ZIF-67 boxes. Moreover, the template-assisted method allows incorporation of functional additives or heteroatoms during synthesis.

2.2.5. Interface Synthesis Method

Interface-assisted synthesis has recently emerged as a powerful strategy to construct sheet-like MOFs with controlled thickness and morphology [49]. In this approach, the reaction is deliberately confined to the boundary between two immiscible phases such as liquid–liquid, liquid–air or liquid–solid interfaces [50]. The restricted environment at the interface slows down isotropic crystal growth and promotes lateral extension. The ultrathin MOFs sheets with high aspect ratios. The interfacial region also provides unique metal ions and organic ligands can assemble in a more ordered fashion. Its precise control over nucleation and growth. The tuning parameters such as interfacial tension, solvent polarity and ligand concentration the crystalline and dimensions of the nanosheets can be tailored. The sheet-like MOFs expose many active sites, facilitate rapid ion diffusion and enhance electron transport. Moreover, the interface synthesis method allows incorporation of functional additives or dopants directly at the boundary. It is additional opportunities to engineer electronic and chemical properties of the nanosheets without compromising their structural stability.

For instance, the preparation of MOFs nanosheets at an air/liquid interface. The morphology and structural characteristics of the nanosheets were strongly influenced by standing time with longer durations producing larger nanosheets. In liquid/liquid systems, two scenarios are typically observed [51]. One involves a biphasic solution in which metal ions and organic ligands are dissolved separately in immiscible solvents. At the interface between these phases, nanosheet formation occurs. Huang group members demonstrated this by dissolving terephthalic acid in an organic solvent while dispersing nickel acetate in water [52]. Two solutions combining light green Ni-MOF nanosheets were generated at the biphasic interface. The versatility of interface synthesis in producing MOFs nanosheets with controlled dimensions and morphologies. It promises a pathway for scalable fabrication of 2D porous materials. Overview of sheet-like MOFs compared to earlier studies (Table 2).

Table 2. Overview of sheet-like MOFs compared to earlier studies.

Materials Name	Ligand	Synthesis Method	Solvent	Temperature/ Time	Applications	Ref.
M-BDC (M = Cu, Mn, Ni and Zr)	Benzene dicarboxylic acid	Oil bath heating method	DMF	135 °C/24 h	Glucose sensing	[53]
DLS-2D-Co-TCPP(Fe)	Tetrakis (4-carboxyphenyl) porphyrin	Sonication method	Ethanol	50 °C/40 min	Nitric oxide sensing	[54]
Zn-TCPP	Tetrakis(4-carboxy phenyl)porphyrin	Sonication method	DMF and ethanol	1 h	-	[40]
HKUST-1	1,3,5-benzenetricarboxylic acid	Stirring method	Ethanol	25 °C/7 h	2D Catalysts	[55]

Table 2. *Cont.*

Materials Name	Ligand	Synthesis Method	Solvent	Temperature/ Time	Applications	Ref.
Cu-TCPP	4,4,4,4-(Porphine-5,10,15,20-tetrayl) tetrakis (benzoic acid)	Stirring method	DMF	90 °C/4 h	-	[56]
Cd-MOF	2-amino terephthalic acid	Water bath method	Tetrahydrofuran	80 °C/1.5 h	Hydrogen production	[57]
Ni–Fe–MOF	1,4-benzenedicarboxylate	Solvothermal method	N,N-dimethylacetamide and water	150 °C/3 h	Water Oxidation	[58]
Ni@NC	2,5 Dihydroxyterephthalic acid	Solvothermal method	DMF, ethanol and water	800 °C/2 h	Microwave Absorption	[59]
Ni-MOF/ Ti_3C_2Tx	Diethyl-2,5-dihydroxyterephthalate	Solvothermal method	DMF and ethanol	80 °C/48 h	Supercapacitor	[60]
Cu-TCPP	Meso-tetra (4-carboxyphenyl) porphine	Magnetic stirring method	DMF	80 °C/4 h	Molecular sieving and antibacterial activity	[61]

2.3. Synthesis of Cubic MOFs Structures

2.3.1. Microwave Assisted Method

Microwave-assisted synthesis has important methods for the synthesis of cubic shaped MOFs due to its ability to accelerate crystallization [62]. This method offers distinct advantages such as selective phase formation, uniform particle size distribution and improved regulation of morphology [63]. Modern microwave reactors are equipped with adjustable power settings, fiber-optic temperature sensors and pressure controllers, fine-tuned reaction environments. The precursor solution is placed in a sealed Teflon vessel and subjected to microwave irradiation at controlled temperature and pressure. The principle behind this technique lies in the interaction of the oscillating electromagnetic field with the dipole moments of molecules in the reaction medium [64]. It induces rotational motion and leads to efficient volumetric heating. The thermal conduction from the vessel walls, microwave energy directly couples with reactant molecules. It is faster reaction rates, reduced energy consumption and enhanced nucleation kinetics.

Park et al. was synthesized a cubic shaped MOFs by using 2,6-naphthalenedicarboxylic acid (NDC) and $Zn(NO_3)_2 \cdot 4H_2O$ (Figure 4a) [65]. The material is constructed from Zn_4O clusters that are interconnected by organic linkers. and the ditopic ligand H_2NDC. These components assemble into a framework that features both micropores and mesopores. The microporous regions arise from cage-like motifs composed of four Zn_4O clusters, two NDC units and four BTB (1,3,5-tris(4-carboxyphenyl)benzene) linkers. The larger mesoporous dodecahedral cages are generated from $[Zn_4O]^{6+}$ clusters combined with eight BTB and four NDC units. The architecture is defined by the coordination of ligands around Zn^{2+} centers and the way these units pack together within the framework. This microwave processing not only shortens synthesis time but also enables precise morphological control.

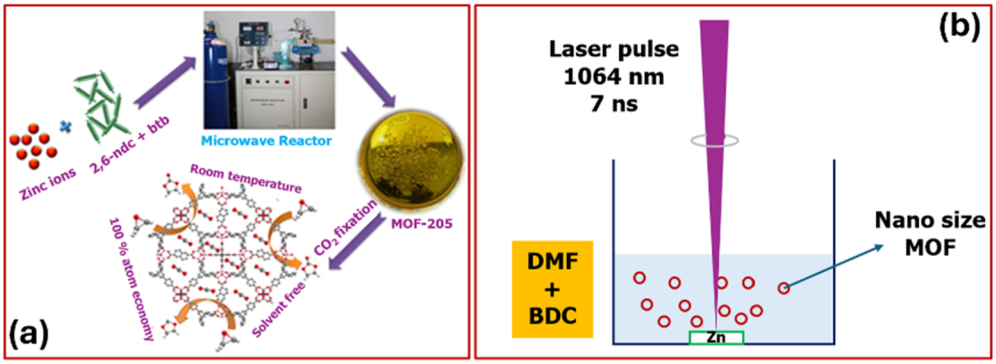

Figure 4. (**a**) Microwave assisted with cubic shaped MOF-205 synthesis. Reproduced with permission [65]. Copyright 2016, American Chemical Society. (**b**) The synthesis of cubic shaped MOFs by using pulsed laser ablation method [66].

2.3.2. Solvothermal Method

Solvothermal synthesis has become a powerful method to accelerate the discovery of cubic MOF structures and refine reaction protocols. The preparation of MOF-5 with cubic morphology, where zinc nitrate hexahydrate and terephthalic acid were employed as precursors. These reagents were dissolved in solvents such as DMF or DEF and the solution was subjected to controlled heating. Subsequent thermal treatment at elevated temperatures yielded cubic MOF-5 crystals. It is very important solvent selection was found to influence crystal growth. It

produces either dense or porous mesocrystal-like frameworks. Interestingly, these MOF-5 crystals could serve as templates for generating cubic ZnO architectures. During pyrolysis, dense MOF-5 converted into cracked ZnO particles, whereas porous MOF-5 relaxed more effectively against volume shrinkage in crack-free cubic ZnO.

Similarly, solvothermal approach for cubic MOF-5 synthesis using a two-step process. In this case, zinc nitrate hexahydrate and 1,4-benzenedicarboxylic acid as a starting material dissolved in DEF [67]. Then, 4-(dodecyloxy)benzoic acid was added to the same solution. The reaction mixture was heated by using oil bath. After completing the reaction, pale-yellow crystals were obtained. This procedure successfully produced cubic MOF-5 crystals. It highlights variations in precursor composition, solvent choice and thermal treatment can be systematically tuned to achieve well-defined morphologies.

2.3.3. Pulsed Laser Ablation Method

Pulsed laser ablation (PLA) method in liquid media has emerged as a distinctive bottom-up physical approach for synthesizing cubic shaped MOFs. It offers an alternative to conventional thermal or chemical methods. In this technique, intense laser pulses strike a solid target submerged in a solvent, releasing nanostructured fragments that subsequently assemble into framework architectures [68]. The structures can be tuned by adjusting parameters such as laser wavelength, pulse duration, spot size and fluence. It modifies the properties in liquid medium including its composition, temperature and density [69]. PLA is considered a rapid and environmentally benign process, as it generates nanostructures without producing harmful byproducts and requires only short reaction times.

The preparation of MOF-5 using a high-purity zinc target irradiated by a pulsed Nd:YAG laser in a DMF solution containing terephthalic acid (Figure 4b) [66]. The particle size of the MOF-5 nanostructures decreased as laser fluence increased, while higher ligand concentrations in the solvent promoted greater yields of nanostructures. The synthesis proceeded at room temperature through the self-assembly of primary building units generated during ablation. The zinc target was placed at the bottom of a beaker filled with DMF, then exposed to 5000 laser pulses under magnetic stirring. The ablated zinc ions interacted within the plasma plume to form coordination bonds with terephthalic acid, yielding porous MOF-5 crystals. The laser energy and ligand concentration directly influence crystal size, morphology and porosity.

2.3.4. Electrochemical Method

Electrochemical synthesis of cubic-shaped MOFs represents a distinctive approach. In this method, metal ions are generated continuously through anodic dissolution rather than being supplied from conventional metal salts [70]. These ions coordinate with organic linkers in the presence of a conducting medium to form the framework. The use of protic solvents helps suppress unwanted metal deposition on the cathode, though hydrogen gas is typically released during the process. This method offers several advantages, mild operating conditions, straightforward control and a cleaner synthesis environment compared to traditional techniques [71].

The preparation of MOF-5 using zinc as the anodic source. The zinc tablet was immersed in a DMF solution containing terephthalic acid [72]. Zinc nitrate was then added in small amounts to increase the ion concentration and shorten the induction period of coordination. Zinc served as the anode and a titanium sheet as the cathode by using a direct current setup. During the reaction, a white precipitate (MOF-5) formed. The MOF-5 was further incorporated into a carbon paste electrode by mixing with spectroscopic carbon powder and liquid paraffin. It produces a modified electrode with enhanced properties compared to the unmodified version. The framework structure was stabilized by coordination between Zn^{2+} ions and terephthalate ligands forms an extended network. To minimize zinc spalling and suppress hydrogen or oxygen evolution at the electrodes, ionic liquid electrolytes were introduced. It offers improved stability during the electrochemical process.

2.3.5. Sonication Method

Sonication synthesis has emerged as a powerful alternative to conventional solvothermal methods. It offers accelerated nucleation and shorter crystallization times that yield smaller particle sizes. In this approach, a precursor solution for the desired MOFs is placed in a horn-type Pyrex reactor connected to a sonicator bar with adjustable power. Ultrasound waves pass through the liquid, bubbles form and collapse in a process known as acoustic cavitation [73]. Compared to traditional heating methods, ultrasound irradiation provides faster synthesis, better control over particle dimensions and improved energy efficiency. Sonochemistry has been widely applied to fabricate nanoscale materials including noble metals, colloids, oxides, chalcogenides, carbides, semiconductors and graphite-based compounds. Its uniqueness lies in the implosive collapse of cavitation bubbles, it produces shockwaves and microjets at solid–liquid interfaces, enhancing mass transfer and reaction activity. High-intensity ultrasound is therefore considered a versatile, eco-friendly and efficient tool for generating nanostructured materials that are often difficult

to obtain by conventional methods. Safarifard and Morsali was synthesized nanostructured cubic shaped MOFs using zinc(II) acetate dihydrate, amino-terephthalic acid (NH_2-BDC) and a rigid bipyridyl ligand (4-bpdh) in DMF [74]. The efficiency of ultrasound-assisted synthesis in reducing reaction time and producing nanoscale MOFs. The cube-shaped MOFs referenced in previously published work revealed in Table 3.

Table 3. Collection of cube-shaped MOFs referenced in previously published work.

Materials Name	Ligand	Synthesis Method	Solvent	Temperature/ Time	Applications	Ref
MOF-205	2,6-naphthalenedicarboxylic acid	Microwave-Assisted method	DMF	150 °C/20 min	CO_2 Fixation	[65]
NH_2-Ce-BDC	2-Aminotropic acid	Calcined method	-	350 °C/2 h	Catalysts	[75]
TMU-16-NH_2	amino-1,4-benzenedicarboxylate	Ultrasound-assisted method	DMF	-	-	[74]
MOF-5	terephthalic acid	Solvothermal method	DMF	150 °C/3 h	-	[76]
Ce-MOF-808	Benzene-1,3,5-tricarboxylic acid	Stirring method	DMF and formic acid	100 °C/15 min	-	[77]
MOF-5	1,4 benzenedicarboxylic acid	Solvothermal method	DEF	150 °C/20 min	-	[67]
UTSA-36a	4 (4-pyridyl) benzoic acid	Solvothermal method	DMF	90 °C/24 h	Gas separation	[78]
Zn-CA-MOFs	Citric acid	Hydrothermal method	Water	160 °C/24 h	catalyst	[79]
MOF-5	1,4 benzenedicar boxylic acid	Laser ablation method	DMF	-	-	[66]
MOF-5	Terephthalic acid	Electro-chemical synthesis	DMF	-	Hydrogen evolution reaction	[72]

2.4. Synthesis of Octahedral MOFs Structures

2.4.1. Co-Precipitation Method

The Co-precipitation method was used to prepare an octahedral shaped MOF. It can be prepared through metal salts and organic linkers are introduced simultaneously into a solvent mixture under controlled conditions. The precipitation of metal ions with the ligand promotes uniform crystal growth, while careful adjustment of concentration and stirring speed favors the development of octahedral morphology. It offers a simple and scalable route to MOFs with well-defined shapes, high porosity and tunable structural features. Mu and Their colleagues revealed that octahedral MOFs (NENU-5) and their derivatives are effective supports owing to their large surface area and good electrical conductivity. NENU-5 exhibits a well-defined octahedral morphology with high porosity [80].

2.4.2. Green Synthesis Method

The green synthesis of MOFs has attracted considerable attention due to its potential to lower energy costs and improve safety [81]. The use of more delicate precursors that might degrade under harsher conditions. While most reported low-temperature strategies have focused on divalent metal carboxylate frameworks. These materials often suffer from poor chemical stability, particularly exposed to moisture, limits their practical utility. Interestingly, ambient synthesis can also introduce low-temperature induced defects. The trivalent metal carboxylate MOFs (e.g., Fe, Al, Cr) generally exhibit greater strongness, especially those based on Al^{3+} and Cr^{3+} (Figure 5a) [82]. However, their chemistry is more complex and establishing versatile room-temperature methods. Despite significant progress, only a limited number of trivalent MOFs have been successfully synthesized under ambient conditions with green solvents including MIL-53(Al), MIL-88A(Fe) and MIL-100(Fe). Extending this concept to tetravalent metals has opened new opportunities. This method not only produced crystalline, chemically stable structures but also allowed particle size control at the nanoscale by tuning reaction parameters.

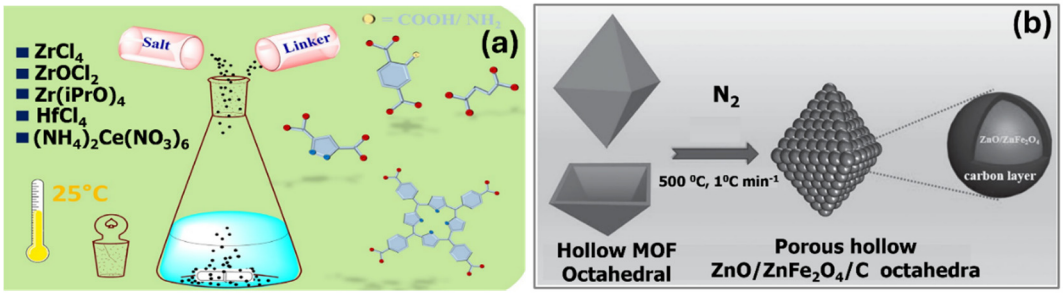

Figure 5. (**a**) Schematic diagram of the room temperature one-step approach. Reproduced with permission [82]. Copyright 2020, John Wiley and Sons. (**b**) The preparation of porous hollow ZnO/$ZnFe_2O_4$/C octahedra. Reproduced with permission [83]. Copyright 2014, John Wiley and Sons.

2.4.3. Refluxing Method

Huang and co-workers demonstrated the synthesis of octahedral Fe(III) MOF-5 using a modified refluxing method [83]. The synthesized MOFs were obtained a hollow porous ZnO/$ZnFe_2O_4$/C octahedra (Figure 5b). During annealing, ultrafine ZnO and $ZnFe_2O_4$ nanocrystals were generated and embedded within a three-dimensional porous carbon framework formed through *in situ* carbonization of the organic ligands. This process produced uniform hollow octahedra stabilized by carbon with ZnO/$ZnFe_2O_4$ nanoparticles as structural building blocks. The architecture integrates a hollow interior, nanoscale crystallites, a conductive and elastic carbon buffer and high porosity. These features impart excellent electrochemical performance including high reversible capacity and superior cycling stability. The synthesis method is straightforward, cost-effective and scalable, making it a promising method for producing advanced functional materials on a larger scale.

2.4.4. Hydrothermal Method

Huang et al., reported the fabrication of porous CuO hollow octahedra using MOFs as templates [84]. A modified hydrothermal method was employed to prepare highly uniform Cu–btc MOFs with well-defined octahedral morphology. The carbon generated during this stage acted as a temporary buffer, helping to preserve the octahedral framework. An annealing step in flowing air at the same temperature completed the transformation into CuO hollow octahedra. The CuO structures combined several advantages, hollow interiors, nanoscale building blocks and high porosity. The evaluated as electrodes for lithium-ion batteries, these materials demonstrated excellent cycling stability and rate capability. Importantly, this method is both cost-effective and scalable. It can be extended to the synthesis of other anisotropic hollow metal oxides with controlled architectures for energy storage and conversion applications.

2.4.5. Microwave-Assisted Method

The microwave-assisted method was used to synthesize an octahedral shaped MOF. This method was efficiently carried out using rapid and uniform heating, which accelerates nucleation and crystal growth. In this method, metal salts and organic linkers are dissolved in a polar solvent such as DMF, then exposed to microwave irradiation. The electromagnetic field interacts with the solvent molecules, producing localized superheating that promotes immediate coordination between metal centers and carboxylate groups. This fast energy transfer reduces induction time, leading to simultaneous nucleation events that favor symmetrical octahedral morphology. As the reaction proceeds, controlled microwave pulses maintain uniform temperature distribution, preventing irregular crystal growth and ensuring high porosity. The mechanism relies on the balance between rapid nucleation and moderated crystal growth, in well-defined octahedral MOFs with tunable structural features.

Khieu and their group members developed porous octahedral ZnO/CuO composites using Zn/Cu-based MOFs (MOF-199) as precursors [85]. The ZnO/CuO composite derived from MOF-199 exhibited a porous octahedral morphology with particle sizes ranging from 5 to 10 μm, forming a hierarchical three-dimensional structure. This architecture was demonstrated excellent activity under visible-light irradiation for the photocatalytic degradation of organic dyes. This microwave approach offers a scalable, energy-efficient pathway for producing advanced MOFs without the need for prolonged solvothermal treatment.

2.4.6. *In-Situ* Synthesis Method

Huo and co-workers highlighted that the rational design of heterogeneous photocatalysts has become a major focus in recent years. $ZnIn_2S_4$/MOF-808 composites were synthesized through an *in-situ* method by combining three-dimensional $ZnIn_2S_4$ microspheres with octahedral MOF-808 [86]. $ZnIn_2S_4$ precursors of different sizes were prepared and specific amounts of MOF-808 were added to the precursor solution, stirred and then transferred into a high-pressure reactor at 160 °C for 10 h. The products were washed with water and ethanol, dried under vacuum and designated according to the MOF-808 loading ratio. A control sample of pure $ZnIn_2S_4$ was synthesized under identical conditions without MOF-808 addition.

2.4.7. Calcination Method

Octahedral MOFs can be transformed into stable, catalytically active derivatives through controlled calcination methods. The organic linkers are gradually decomposed to yield porous metal oxides while retaining the parent framework geometry. The synthesized octahedral crystals are subjected to stepwise heating under chosen atmospheres, allowing the removal of ligands without collapsing the structural integrity. This thermal

treatment not only preserves octahedral morphology but also introduces defects and oxygen vacancies that enhance catalytic potential. Tuning parameters such as temperature ramp rate, holding time and ambient gas composition.

Zhang and co-workers demonstrated that an octahedral shaped Cu-BTC derivatives can be obtained through direct calcination of copper-based MOFs under different atmospheric conditions [87]. Cu-BTC crystals were synthesized hydrothermally by combining benzene-1,3,5-tricarboxylic acid in ethanol with $Cu(NO_3)_2 \cdot 3H_2O$ in water, followed by stirring and treatment at 140 °C for 24 h. The crystals were washed, dried and then calcined at 250 °C for two hours under different atmospheres (CO, O_2, H_2, Ar), yielding Cu-BTC-CO, Cu-BTC-O, Cu-BTC-H and Cu-BTC-Ar derivatives. Calcination is a versatile method for converting octahedral MOFs into functional materials with improved stability and catalytic performance. Summary of the octahedral-form MOFs described in previous work (Table 4).

Table 4. Summary of the octahedral-form MOFs described in previous work.

Materials Name	Ligand	Synthesis Method	Solvent	Temperature/ Time	Applications	Ref
NENU-5	L-glutamic acid	Stirring method	Water and ethanol	RT/14 h	Hydrogen evolution	[80]
Zinc(II) MOF	Glutaric acid	Microwave method	Water	800W/10 min	Dye Degradation	[88]
MOF-801	Fumaric acid	Stirring method	Formic acid and water	RT/12 h	-	[82]
NH_2-MIL-125(Ti)	2-Amino-1,4-benzenedi-carboxylic acid	Solvothermal method	DMF and methanol	150 °C/24 h	-	[89]
CuO hollow octahedra	Benzene 1,3,5-tricarboxylate)	Hydrothermal method	Methanol	300 °C/1 h	Lithium-ion battery	[84]
MOF-199	Benzene-1,3,5-tricarboxylate	Microwave method	Ethanol, water and DMF	250W/30 min	Photocatalytic Degradation	[85]
Fe/Eu-MOF	2-aminoterephthalic acid	Solvothermal method	DMF	120 °C/20 h	Sensing application	[90]
$ZnIn_2S_4$/MOF-808	Trimesic acid	Solvothermal method	DMF and formic acid	120 °C/48 h	Photocatalyst	[86]
Ce-BDC MOF	1,4-benzenedicarboxylic acid	Solvothermal method	DMF-formic acid	60 °C/2 h	N_2O decomposition	[91]
HKUST-1	Benzene-1,3,5-tricarboxylic acid	Ultrasonication method	Methanol	RT/3 h	Capacitor applications	[92]

3. Different Synthetic Methods Impact the Morphology of MOFs

The morphology of MOFs is highly dependent on the synthetic methods employed with each method imparting distinct structural characteristics. *In-situ* electrochemical synthesis often yields uniform nanostructures with controlled crystallinity. Meanwhile, hydrothermal and solvothermal methods enable the formation of well-defined cubic and octahedral crystals through slow nucleation and growth under high temperature and pressure. Microwave-assisted synthesis accelerates crystallization producing smaller particles with tunable shapes. Whereas, sonication promotes rapid nucleation, often in rod-like or sheet-like morphologies. Surfactant-assisted and regulator-assisted methods provide additional control over particle size and shape by modulating surface energies and growth kinetics. Template-assisted synthesis allows for the replication of predefined architectures, leading to hierarchical or porous morphologies, while interface synthesis exploits phase boundaries to generate unique nanosheet structures. Pulsed laser ablation, though less conventional, can produce highly dispersed nanoparticles with novel morphologies due to rapid plasma-induced reactions. These diverse synthetic strategies highlight the critical role of methodology in tailoring MOFs morphology, thereby enabling precise control over their physicochemical properties.

MOFs with certain morphologies exhibit different properties because structure directly dictates function. The dimensionality and shape of a MOF, whether 1D (rods), 2D (sheets) or 3D (Cubic and Octahedral) frameworks control factors such as surface area, porosity, diffusion pathways, stability and anisotropy, all of which influence performance in applications. 1D rod-like structures growth along a single axis creates anisotropic properties, improving ion or electron transport and making them valuable in membranes and photocatalysis. 2D sheets, ultrathin layers provide exceptionally high surface area and short diffusion paths, which are ideal for gas separation, sensing and energy storage. 3D frameworks (cubic or octahedral) highly crystalline morphologies offer interconnected pore networks and mechanical strongness, making them excellent for gas storage, separation and optoelectronic applications. In essence, morphology determines molecules interact with the framework whether through diffusion, adsorption or catalytic sites. MOFs with different morphologies show distinct properties and tailoring morphology through synthetic methods is a powerful strategy for designing MOFs with application-specific performance. The summary of all synthesis methods for different MOFs morphologies is presented in Table 5.

Table 5. Overview of synthesis methods to impact MOFs morphologies.

Synthetic Method	Impact on Morphology	Examples
In-Situ Electrochemical Method	Produces uniform nanostructures with controlled crystalline and fine particle sizes.	Often used for thin films and coatings, morphology depends on applied potential.
Hydrothermal Method	Yields well-defined cubic and octahedral crystals through slow nucleation under pressure.	Common for large single crystals, widely used in gas storage MOFs.
Solvothermal Method	Enables diverse morphologies (cubic, rod-like, sheet-like) depending on solvent system.	Solvent polarity strongly influences particle shape.
Microwave-Assisted Method	Accelerates crystallization in smaller particles with tunable shapes.	Produces nanoscale MOFs quickly, energy-efficient synthesis.
Sonication Method	Promoting rapid nucleation often generates rod-like or sheet-like morphologies.	Useful for exfoliating layered MOFs into nanosheets.
Surfactant-Assisted Method	Controls particle size and shape by modifying surface energies, enables hierarchical forms.	Surfactants act as structure-directing agents; useful for porous morphologies.
Regulator-Assisted Method	Provides fine control overgrowth kinetics, yields uniform and size-controlled crystals.	Regulators (e.g., acids/bases) tune nucleation rates and particle dimensions.
Template-Assisted Method	Replicates predefined architecture, produces porous or hierarchical morphologies.	Templates like polymers or silica guide MOFs growth into specific shapes.
Interface Synthesis Method	Exploits phase boundaries, generates nanosheet or layered structures.	Often used for 2D MOFs, liquid–liquid interfaces stabilize sheet-like growth.
Pulsed Laser Ablation Method	Produces highly dispersed nanoparticles, unique morphologies through plasma-induced reactions.	Less conventional, enables ultrafine MOFs particles with novel surface features.

4. Applications for MOFs with Different Morphology

4.1. Applications for Rod-Like MOFs Structures

4.1.1. Supercapacitor Applications

MOFs promising candidates for electrode applications in energy storage systems. Since the first MOFs were reported in 1995, research in this field has expanded rapidly with more than 20,000 distinct MOFs structures now documented [93]. In a related study, Chen and co-workers achieved the *in-situ* electrochemical synthesis of rod-like Ni-MOFs directly on nickel foam (NF) substrates [28]. During this process, the NF acted as the Ni^{2+} source, trimesic acid served as the organic ligand and NH_4F functioned as the supporting electrolyte. The Ni-MOFs were grown directly on the NF surface, eliminating the need for binders or additional treatments. The optimized Ni-MOF/NF electrode exhibited a high specific capacity of 5.11 C cm^{-2} at 2 mA cm^{-2} and retained 57.1% capacity even at 30 mA cm^{-2}, highlighting its excellent rate capability. The rod-like arrays self-assembled into flower-like structures, further enhancing electrochemical performance. Moreover, the Ni-MOF-1h//AC hybrid supercapacitor delivered an impressive energy density of 586.7 mWh cm^{-2} at a power density of 3679 mW cm^{-2}. The potential of MOF-based electrodes in high-performance energy storage applications.

4.1.2. CO_2 Adsorption Applications

The selective adsorption of CO_2 over N_2 in MOFs has attracted significant interest due to its relevance in post-combustion carbon capture and storage [94]. Enhancing CO_2/N_2 selectivity has been achieved through strategies that exploit the higher polarizability and quadrupole moment of CO_2 compared with N_2, stronger interactions between CO_2 molecules and the internal surfaces of MOFs. More recently, kinetic separation approaches have been introduced, offering moderate CO_2 adsorption enthalpies alongside excellent selectivity. However, separation performance evaluated under ambient conditions and the thermal and chemical stability of MOFs is critical, particularly since many carboxylate-based frameworks are prone to hydrolysis. Tang and co-workers synthesized rod-like MIL-53(Al) using a microwave-assisted solvothermal method to improve CO_2 adsorption [31]. MOFs, composed of metal centers coordinated with organic ligands, are well suited for gas capture because of their high surface area and narrow pore size distribution. The optimized sample prepared under stirring at 130 °C, 200 W and 3 h exhibited high crystallinity and rod-like morphology.

4.1.3. Catalyst Applications

MOFs possess a high surface areas and tunable porosity but suffer from poor conductivity and fewer active sites. MOFs with metal oxides and composite materials can be engineered to integrate the strengths of both systems enhanced surface area from MOFs and abundant catalytic sites from oxides [95]. This synergistic interaction effectively bridges the shortcomings of each individual framework that improved catalytic performance. In recent years, two-dimensional (2D) nanostructures have gained significant attention due to their superior properties compared to bulk materials. Nanorods often exhibit higher activity than nanoparticles, a phenomenon attributed to

differences in exposed crystal planes and the density of active sites. Photodegradation of toxic dyes in aqueous media using renewable and freely available energy sources offers a sustainable approach. This process degrades pollutants into less harmful compounds or achieves complete mineralization.

Dhak and co-workers reported the rod-like Fe–Al bimetallic MOFs for efficient fluoride adsorption and photocatalytic degradation of carcinogenic dyes [38]. MOFs containing trivalent metals such as Al^{3+}, Cr^{3+} and Fe^{3+} were shown to degrade methylene blue under Xe lamp irradiation. The Fe–Al bimetallic MOF synthesized with terephthalic acid (BDC) as a linker in DMF medium. It referred to as Fe–Al BDC, combined high thermal and chemical stability with a porous structure and large surface area. This material was successfully applied for solar-driven photodegradation of hazardous dyes such as rhodamine B, methylene blue and other xanthene derivatives. Furthermore, its performance in fluoride removal and dye degradation was evaluated under varying conditions such as pollutant concentration, contact time, dosage, solution pH and temperature. The study also considered the presence of competing anions, reusability and tests with real water samples. It confirms its potential as a multifunctional material for environmental remediation.

4.1.4. Sensor Applications

In recent years, transition metals have been widely employed in the construction of MOFs due to their ability to form secondary building units (SBUs) with well-defined geometries, which are essential for predictable framework topologies [96]. Calcium has also emerged as an attractive alternative metal source because of its abundance, low cost, biocompatibility and eco-friendly nature. Developing a simple and scalable method for synthesizing calcium-based MOFs. The variability in calcium coordination geometry and its tendency to form diverse infinite SBUs complicate structural control. Huang and co-workers reporting an ultrafast, large-scale synthesis of calcium MOFs with rod like SBUs, alongside their application in luminescence detection of water in organic solvents [39]. Ca-MOFs demonstrated excellent sensitivity for detecting water in commercial solvents such as DMF, ethanol and THF with a limit of detection (LOD) around 1%. The synthesis employed di- and tritopic carboxylate ligands with calcium acetate chosen as the precursor due to its poor solubility in organic solvents and rapid precipitation behavior. The controlling water content during synthesis is very important, the crystallinity of Ca-MOFs was preserved. Ca-MOFs material exhibited fast luminescence response and reliable water detection capability. The potential of calcium MOFs as scalable, multifunctional materials for both environmental monitoring and advanced applications.

4.2. Applications for Sheet-Like MOFs Structures

4.2.1. Sensor Applications

The sheet-like MOFs exhibit unique physical and chemical characteristics arising from their thin structures, large surface areas and high surface-to-volume ratios [97]. Zhou and his colleagues reported a sheet-on-sheet (SOS) assembly of MOFs/graphene hybrids for nitric oxide (NO) sensing at room temperature [54]. Detecting level, NO with chemiresistive sensors under ambient conditions is challenging due to the need for both high sensitivity and stability. Their design employed a porphyrin-based MOF (DLS-2D-Co-TCPP(Fe)) combined with 5-aminonaphthalene-1-sulfonic acid-modified reduced graphene oxide (ANS–rGO) nanosheets through coordination interactions. The SOS heterojunction sensor exhibited outstanding NO-sensing properties including high sensitivity, repeatability, selectivity and rapid response/recovery. The superior performance was attributed to the integration of NO-responsive Fe–N_4 active units within MOF nanosheets and the heterojunction architecture, which facilitated efficient carrier migration.

4.2.2. Supercapacitor Applications

MOFs formed through the self-assembly of metal ions or clusters with multifunctional organic ligands. It has been widely utilized as precursors for synthesizing advanced carbon materials. Typically, carbon nanostructures doped with heteroatoms such as nitrogen, phosphorus or sulfur are obtained by pyrolyzing MOFs under controlled atmospheres at suitable temperatures. These heteroatom-doped carbons exhibit several advantages including tailored morphologies, large internal surface areas, high crystallinity, accessible pore networks and excellent electronic conductivity. Importantly, the incorporation of heteroatoms can modulate the electronic structure of carbon, thereby enhancing conductivity, hydrophilicity and overall performance in electrochemical reactions.

Liu and co-workers prepared sheet-like phosphorus-doped porous carbons derived from Co-MOFs for use as supercapacitor electrodes [98]. The material (P-C-600) obtained via thermal treatment of Co-MOF powders, benefited from both its sheet-like microstructure and the inherent phosphorus content of the precursor. These

features enabled rapid ion transport and improved rate capability. The P-C-600 electrodes delivered a specific capacitance of 168 F g^{-1} at 1.0 A g^{-1}. It retained approximately 97% of their initial capacitance after 3000 charge–discharge cycles at 20 A g^{-1}, demonstrating excellent cycling stability.

4.2.3. Catalysts Applications

In catalytic applications, MOFs can be utilized through three primary strategies, the inorganic nodes within MOFs act as intrinsic catalytic sites. The external functional species can be incorporated either on the surface or within the framework. MOFs serve as solid precursors for metal or metal oxide catalysts due to their high metal content and ease of transformation. Meanwhile, the inherently low electronic conductivity of MOFs and the partial blockage of active metal sites by organic ligands restrict their efficiency, particularly in reactions such as water oxidation at ultra-high current densities [99]. Furthermore, during high-temperature pyrolysis, the loss of organic ligands often compromises the intrinsic framework reducing the structural integrity of MOF-derived electrocatalysts. The designing of MOFs based and MOFs derived materials with abundant electrocatalytically active nano and microstructures are being actively explored. Recent studies highlight that MOFs with sheet-like morphologies exhibit superior electrochemical performance compared to bulk structures. Their nanometer-scale thickness facilitates rapid ion and electron transport, while exposing a greater number of accessible active sites.

Zhan and Zeng developed a 2D nanosheets (copper-based MOFs) acted as self-templating precursors, transforming into CuO, CuO–Cu_2O composites or metallic Cu and served as versatile supports for noble metal nanoparticles [55]. Anchoring Au, Ag, Pt or Pd on their surfaces enhanced catalytic activity in CO_2 hydrogenation and 4-nitrophenol reduction. Under H_2/Ar reduction, Cu^{2+} ions converted into uniformly distributed Cu nanoparticles on carbon supports, while free carboxyl groups facilitated noble metal immobilization. These MOF-derived copper systems demonstrated strong catalytic performance in both gas-phase CO_2 hydrogenation and liquid-phase 4-nitrophenol reduction. The potential of shape-controlled synthesis for multifunctional catalyst design.

In electrocatalyst, Chen and his co-workers developed cobalt-based MOFs with sheet-like architecture through a solvothermal method, achieving high efficiency in electrocatalytic oxygen evolution [100]. The Co-MOFs delivered ultra-high current densities for water oxidation under mild alkaline conditions and maintained excellent durability after 10,000 cyclic voltammetry scans. Their sheet-like morphology improved conductivity and maximized cobalt active site exposure, while sulfur incorporation provided synergistic effects through Co, N, C, O and S interactions. These features highlight the potential of sheet-like Co-MOFs as strong, non-precious electrocatalysts for industrial water splitting.

Wang and co-workers synthesized a MOF-derived CdS–MoS_2 composite with sheet-assembled, flower-like morphology for visible-light hydrogen production [57]. The material exhibited a large surface area, tunable morphology and abundant catalytic sites, which enhanced photocatalytic activity. Under simulated light with lactic acid as a sacrificial agent, the optimized composite achieved a hydrogen evolution rate of 41.8 mmol g^{-1} h^{-1}, nearly 47 times higher than pure CdS. Incorporation of MoS_2 suppressed electron–hole recombination and shifted the conduction band, accelerating water reduction. The synergistic combination of CdS and MoS_2 demonstrates that MOF-derived composites can significantly improve photocatalytic hydrogen generation.

4.3. Applications for Cubic MOFs Structures

4.3.1. Catalytic Applications

MOFs have attracted significant attention as heterogeneous catalysts for this transformation. Their advantages include high surface area, ordered pore networks, tunable particle size and porosity, strong CO_2 adsorption capacity and abundant acidic/basic sites. Park and co-workers synthesized cubic MOFs via a microwave-assisted method and demonstrated their catalytic efficiency in solvent-free CO_2 fixation to cyclic carbonates [65]. The bromide ions from tetrabutylammonium bromide initiate epoxide ring opening. The alkoxide intermediate subsequently attacks the carbon atom of CO_2 forming a carbonate species. Ring closure then occurs through intramolecular attack of the carbonate oxygen on the C–Br bond. On the other hand, electrocatalysis provides an efficient pathway for converting electrical energy into chemical energy, encompassing key processes such as the oxygen reduction reaction (ORR), carbon dioxide reduction (CO_2RR) and electro-organic transformations.

Jiang and co-workers developed cube-like Ce MOF-derived Pt/CeO_2 catalysts that showed excellent activity for HCHO oxidation [75]. Pyrolysis of MOFs generated oxides with high porosity and structural defects, which acted as anchoring sites for Pt nanoparticles and enhanced catalytic efficiency. The oxidation mechanism involved reactive oxygen species converting HCHO into intermediates that decomposed into H_2O and CO_2. Surface hydroperoxyl groups facilitated adsorption, while strong Pt–CeO_2 interactions activated oxygen species. Oxygen vacancies provided both sites for oxygen activation and dispersion centers for Pt in superior catalytic performance

compared with conventional Pt/CeO_2. Morphology-controlled Pt/CeO_2 offered larger surface area, higher vacancy concentration and improved Pt deposition, delivering outstanding activity for HCHO oxidation. The MOFs synthesis via an electrochemical approach and applied them to the hydrogen evolution reaction. Incorporation of MOF-5 into a carbon paste electrode significantly enhanced catalytic activity. It shows improved hydrogen atom oxidation and desorption compared to the unmodified electrode. Cyclic voltammetry in ionic liquid revealed quasi-reversible redox processes at Zn centers, while sulfur incorporation further boosted performance. The MOF-derived system demonstrated superior electrocatalytic efficiency and durability, highlighting its potential as a flexible platform for advanced HER catalyst design.

4.3.2. Gas Separation Applications

Gas separation is an essential industrial process widely applied in areas such as natural gas and biogas purification, oxygen–nitrogen separation from air, carbon dioxide capture and hydrogen production for clean energy [101]. MOFs have emerged as highly promising candidates for gas separation due to their structural versatility. Their design allows pore sizes to be tailored by modifying organic linkers, while the flexible framework of certain MOFs enables dynamic tuning of pores under varying pressure or temperature. This adaptability provides MOFs with unique advantages over conventional porous materials. Chen and co-workers explored a primitive cubic MOFs network with exceptional selectivity for small hydrocarbon molecules [78]. The three-dimensional, doubly interpenetrated framework $Zn_2(PBA)_2(BDC)\cdot(DMF)_3(H_2O)_4$ (UTSA-36) was constructed via self-assembly of pyridylcarboxylate and bicarboxylate linkers coordinated to paddle-wheel $Zn_2(COO)_4$ units. Activated UTSA-36 demonstrated highly selective adsorption of C_2 hydrocarbons (C_2H_6, C_2H_4, and C_2H_2) over methane. This performance was attributed to its unique three-dimensional intersected pore structure. Its potential is a valuable microporous material for industrially important separations of C_2 hydrocarbons from methane.

4.4. Applications for Octahedral MOFs Structures

4.4.1. Catalytic Applications

MOFs and coordination polymers (CPs) are highly appealing materials due to their tunable crystalline structures and versatile functionalities. It offers broad opportunities for the development of advanced functional systems. Among their unique features, structural transformations particularly single-crystal to single-crystal (SCSC) conversions are of great interest because they often occur cooperatively and can introduce novel properties. These transformations may be triggered by external stimuli including light, solvents, guest adsorption–desorption or chemical reactions. In many cases, SCSC processes alter the coordination geometry of the metal centers, leading to changes in material properties such as optical behavior or catalytic activity.

Mu and co-workers demonstrated this by synthesizing octahedral MOF-derived carbon supports decorated with PtCu nanoalloys for HER [80]. Through a confined replacement reaction followed by carbonization, uniformly dispersed PtCu nanoparticles were embedded within the porous MOF-derived carbon matrix. The catalyst (PtCu–MoO_2@C) exhibited remarkable HER activity, requiring only a low overpotential of 24 mV at 10 mA cm^{-2} in alkaline media, outperforming commercial Pt/C. Furthermore, the catalyst displayed excellent mass activity and long-term durability. The effectiveness of MOFs-assisted synthesis in producing highly active and stable PtCu nanoalloy composites for hydrogen evolution.

Yimklan et al. reported a ligand-substitution-induced SCSC transformation in a rectangular Zn(II) MOF, where the framework converted from octahedral to tetrahedral geometry [88]. In this system, the aromatic ring of 4,4′-bipyridine acted as a light-harvesting unit, absorbing UV-C radiation and transferring energy to adjacent Zn trinuclear clusters. Excited electrons were generated in the conduction band while holes formed in the valence band, producing reactive hydroxyl radicals (•OH). These radicals rapidly degraded methyl orange (MO) into smaller molecules such as CO_2 and H_2O. Electrostatic attraction between the anionic dye and the cationic framework further enhanced dye adsorption, thereby improving photocatalytic efficiency.

Similarly, Khieu and co-workers synthesized a porous octahedral ZnO/CuO composite derived from Zn/Cu-based MOF-199 [85]. The material exhibited a hierarchical three-dimensional structure composed of porous octahedral particles measuring 5–10 μm. Compared with pure ZnO and CuO, the ZnO/CuO composite demonstrated superior photocatalytic degradation of phenol and dyes including methylene blue, methyl orange, phenol red and congo red under visible light. This enhanced activity was attributed to the formation of a stable p–n junction, which facilitated efficient separation of photogenerated electron–hole pairs. The catalyst-maintained stability after four consecutive cycles and its degradation kinetics were consistent with a unimolecular reaction

model combined with Langmuir adsorption behavior. The porous ZnO/CuO composite represents a strong and efficient visible-light-driven photocatalyst with strong potential for treating dye pollutants in wastewater.

Huo and co-workers developed an *in-situ* synthesized S-scheme heterojunction composed of $ZnIn_2S_4$ microspheres and octahedral MOF-808 ($ZnIn_2S_4$/MOF-808) [86]. The study demonstrated that the size of $ZnIn_2S_4$ microspheres significantly influenced photocatalytic performance with optimal activity achieved at a particle size of approximately 6 μm when integrated with MOF-808. Compared with individual $ZnIn_2S_4$ and MOF-808, the composite heterojunction exhibited markedly enhanced CO_2 reduction activity. The optimized $ZnIn_2S_4$/MOF-808 system achieved a CO yield of 8.21 μmol g^{-1} h^{-1}, which was nearly ten times higher than $ZnIn_2S_4$ alone and eight times greater than MOF-808. These findings highlight the effectiveness of S-scheme heterojunctions in boosting photocatalytic CO_2 conversion efficiency through synergistic band alignment and controlled nanostructure design.

4.4.2. Lithium-Ion Batteries Applications

MOFs have proven to be effective templates or precursors for generating novel porous nanoarchitectures with unique properties. However, the development of three-dimensional (3D) MOF-derived porous assemblies as continuous electrode materials for lithium-ion batteries (LIBs). 3D porous electrodes with interconnected carbon networks can provide abundant active sites. It facilitates rapid charge transport and mass diffusion and simultaneously buffers the mechanical stress caused by volume changes during cycling. Huang and co-workers fabricated porous ZnO/$ZnFe_2O_4$/C octahedra with hollow interiors by employing MOFs as both precursors and self-sacrificing templates [83]. The hybrid ZnO/$ZnFe_2O_4$/C material exhibited excellent electrochemical performance as an LIB anode, combining high capacity, superior rate capability and long cycle life. Its outstanding properties stem from the synergistic effects of ultrafine Zn-based oxide nanocrystals, elastic carbon networks, hollow interiors and high porosity. Similarly, Wu and his group members synthesized porous CuO hollow octahedra using a straightforward approach. A Cu–btc MOF template was prepared via hydrothermal synthesis and then decomposed thermally at 300 °C. The CuO hollow structures demonstrated remarkable electrochemical behavior when tested as LIB electrodes, showing stable cycling and strong rate capability. Importantly, this low-cost and convenient strategy can be extended to fabricate other anisotropic hollow metal oxides. The well-defined morphologies, offering broad potential for energy storage and conversion applications.

4.4.3. Sensor Applications

MOFs based sensor applications is attractive because of their stability, tunable porous structures, biocompatibility and cost-effectiveness. The composition and ratio of metal ions and organic ligands, mixed-metal MOFs can be engineered to exhibit adjustable enzyme-like activity and intrinsic fluorescence. The synergistic effects between multiple metals often enhance performance beyond that of single-metal MOFs. Furthermore, the inherent fluorescence of MOFs eliminates the need for external probes, simplifying experimental procedures, reducing costs and improving detection accuracy. Chen et al., reported the synthesis of nano-octahedral bimetallic Fe/Eu-MOFs for dual-mode alkaline phosphatase (ALP) sensing, exploiting both their peroxidase-like activity and fluorescence properties [90]. Since ALP measurement is routinely used in clinical diagnostics, the development of efficient biosensors is of significant biomedical importance. The Fe/Eu-MOF was prepared via a hydrothermal method and demonstrated the ability to catalyze the oxidation of TMB by H_2O_2, producing a blue oxTMB product. Interestingly, oxTMB simultaneously quenched the fluorescence of the MOF, enabling dual-signal detection.

4.4.4. Electrochemical Capacitor Applications

Carbon-based materials such as activated carbon, carbon nanotubes and graphene have been extensively studied as electrode candidates for electrochemical capacitors (ECs). It owing to their large surface area, chemical stability and good conductivity. However, their energy storage mechanism based mainly on reversible ion accumulation at the electrode/electrolyte interface limits the specific capacitance achievable with pure carbon electrodes. Pseudocapacitors have been explored, which store charge through fast and reversible redox reactions involving materials like metal oxides, hydroxides, sulfides and conducting polymers. These systems can deliver higher capacitance and energy density but their poor electrical conductivity often restricts electron transport and reduces rate capability.

MOFs highly ordered crystalline materials composed of metal clusters linked by organic ligands have emerged as versatile templates or precursors for producing porous carbons and metal oxides via thermolysis. Their tunable structures and large surface areas make them particularly attractive for capacitor applications. MOFs derived sulfide–carbon composites with the combined properties of high capacitance, energy density and cycling stability remain relatively rare. Chen et al., developed a MOFs-templated sulfidation strategy to synthesize $Cu_{1.96}S$–

C hybrid composites [92]. The ultrafine $Cu_{1.96}S$ nanoparticles were uniformly embedded within porous carbon octahedra. During the simultaneous sulfidation and carbonization process, the crystalline MOFs precursor reacted with sulfur while retaining its octahedral morphology, yielding a stable porous composite. The tested as EC electrodes, the $Cu_{1.96}S$–C-650 material exhibited high specific capacitance along with excellent cycling durability. It demonstrates the potential of MOF-derived sulfide–carbon hybrids for advanced energy storage applications.

5. Future Prospective

The development of MOFs with diverse morphologies such as rod, sheet, cubic and octahedral structures faces several challenges yet also promising future directions. A major difficulty lies in achieving precise morphological control during synthesis. A small variation in reaction conditions can shift growth from cubic to octahedral or rod forms, complicating reproducibility. Rod-shaped MOFs are advantageous for directional transport and biomedical delivery but face aggregation and dispersion issues. Surface functionalization or polymer embedding could enhance their applicability. Sheet-like MOFs with ultrafast diffusion and high surface exposure are hindered by fragility and restacking tendencies. Future research should focus on stabilizing two-dimensional frameworks through interlayer spacers or flexible substrates.

Cubic MOFs are stable and often suffer from limited external surface area, restricting fast adsorption processes. Future work may focus on hybrid designs that combine cubic stability with surface modifications. Octahedral MOFs present opportunities in facet-driven catalysis. However, their sharp edges and lower mechanical resilience demand strategies for reinforcing structural integrity such as composite formation or hierarchical assembly. The integration of machine learning approaches offers a transformative pathway for tailoring these morphologies to specific functional demands. By leveraging large datasets of synthesis parameters, structural features and performance metrics. Machine learning models can predict optimal conditions for generating desired morphologies and uncover hidden correlations between structure and application. This data-driven strategy not only accelerates the discovery of novel MOFs but also enables rational design for targeted uses in different applications. The synergy between experimental synthesis and computational intelligence. Machine learning can guide researchers toward more efficient, sustainable and application-oriented development of MOFs with precisely engineered morphologies. Finally, the future perspective emphasizes integrating morphology control with advanced synthesis. Its computational design and hybridization approaches tailor MOFs for next-generation applications.

6. Conclusions

In this review, we have discussed the synthesis of MOFs with different morphologies including rod, sheet, cubic and octahedral structures. We highlighted various fabrication strategies such as electrochemical, hydrothermal, solvothermal, microwave-assisted, sonication, surfactant-assisted, regulator-assisted, template-assisted, interface synthesis, pulsed laser ablation, co-precipitation and green synthesis methods. Each morphology not only reflects the influence of synthesis conditions but also dictates the functional performance of MOFs in different applications. Rod-like MOFs provide enhanced adsorption and degradation capabilities, whereas sheet-like architecture delivers high surface area and conductivity. The sheet-like forms for their ultrathin, high-surface-area using for different applications. Cubic frameworks have shown promise in electrocatalysis and gas-related applications, while octahedral structures excel in photocatalysis, hydrogen evolution and electrochemical devices. A comparative evaluation highlights that morphology-driven properties are central to tailoring MOFs for specific applications. Despite these advances, challenges remain in achieving scalable, eco-friendly synthesis methods, precise morphology control and long-term stability under operational conditions. Future research should focus on integrating green chemistry principles and exploring hybrid synthesis approaches. Bridging laboratory-scale innovations with industrial applications to fully harness the potential of MOFs in sustainable technologies.

Author Contributions

S.G.E.: Writing—review & editing, Writing—original draft, Methodology, Investigation, Conceptualization. Y.G.: Writing—review & editing, Visualization, Validation, Supervision, Project administration. A.W.: Writing—review & editing, Visualization, Project administration. All authors have read and agreed to the published version of the manuscript.

Funding

This work was funded by Yangzhou University's State Key Laboratory of Analytical Chemistry for Life Science (No. SKLACLS2001) and the Natural Science Fund for Colleges and Universities in Jiangsu Province (No. 19KJB550002). Thanks to the Yangzhou University Test Center.

Institutional Review Board Statement

Not applicable.

Informed Consent Statement

Not applicable.

Data Availability Statement

Data will be made available on request.

Conflicts of Interest

The authors declare no conflict of interest.

Use of AI and AI-Assisted Technologies

No AI tools were utilized for this paper.

References

1. Wu, J.; Xu, F.; Li, S.; et al. Porous Polymers as Multifunctional Material Platforms toward Task-Specific Applications. *Adv. Mater.* **2019**, *31*, 1802922.
2. Khakbaz, M.; Ghaemi, A.; Sadeghi, G.M.M.; et al. Synthesis Methods of Microporous Organic Polymeric Adsorbents: A Review. *Polym. Chem.* **2021**, *12*, 6962–6997.
3. Bhunia, S.; Deo, K.A.; Gaharwar, A.K.; et al. 2D Covalent Organic Frameworks for Biomedical Applications. *Adv. Funct. Mater.* **2020**, *30*, 2002046.
4. Kidanemariam, A.; Lee, J.; Park, J.; et al. Recent Innovation of Metal-Organic Frameworks for Carbon Dioxide Photocatalytic Reduction. *Polymers* **2019**, *11*, 2090.
5. Luo, Y.; Mei, Y.; Xu, Y.; et al. Hyper-Crosslinked Porous Organic Nanomaterials: Structure-Oriented Design and Catalytic Applications. *Nanomaterials* **2023**, *13*, 2514.
6. Tang, J.; Yang, M.; Dong, W.; et al. Highly Porous Carbons Derived from MOFs for Shape-Stabilized Phase Change Materials with High Storage Capacity and Thermal Conductivity. *RSC Adv.* **2016**, *6*, 40106–40114.
7. Lü, Y.; Zhan, W.; He, Y.; et al. MOF-Templated Synthesis of Porous Co_3O_4 Concave Nanocubes with High Specific Surface Area and Their Gas Sensing Properties. *ACS Appl. Mater. Interfaces* **2014**, *6*, 4186–4195.
8. Shahnawaz Khan, M.; Li, Y.; Li, D.S.; et al. A Review of Metal–Organic Framework (MOF) Materials as an Effective Photocatalyst for Degradation of Organic Pollutants. *Nanoscale Adv.* **2023**, *5*, 6318–6348.
9. Espallargas, G.M.; Coronado, E. Magnetic Functionalities in MOFs: From the Framework to the Pore. *Chem. Soc. Rev.* **2018**, *47*, 533–557.
10. Song, X.; Liu, J.; Zhang, T.; et al. 2D Conductive Metal-Organic Frameworks for Electronics and Spintronics. *Sci. China Chem.* **2020**, *63*, 1391–1401.
11. Kalita, R.; Thadhani, C.; Manna, K.; et al. Architecting Metal–Organic Framework-Based/Derived Catalysts for Methane Functionalization. *ACS Catal.* **2026**, *16*, 882–909.
12. Deng, W.-H.; Xiao, K.; Cheng, Z.; et al. Dimensionally Engineered MOF Films for Chemiresistive Sensors. *Chem. Soc. Rev.* **2026**, *55*, 910–940.
13. Yaghi, O.M. Reticular Chemistry—Construction, Properties, and Precision Reactions of Frameworks. *J. Am. Chem. Soc.* **2016**, *138*, 15507–15509.
14. Kitagawa, S. Metal–Organic Frameworks (MOFs). *Chem. Soc. Rev.* **2014**, *43*, 5415–5418.
15. Gregan, T.; Gregan, J. Artificial Intelligence at the Intersection of Chemistry and Materials Science. *AI* **2026**, *7*, 89.
16. Ye, G.; Chen, C.; Lin, J.; et al. Alkaline Earth-Based Metal–Organic Frameworks for Biomedical Applications. *Dalton Trans.* **2021**, *50*, 17438–17454.
17. Felix Sahayaraj, A.; Joy Prabu, H.; Maniraj, J.; et al. Metal–Organic Frameworks (MOFs): The Next Generation of Materials for Catalysis, Gas Storage, and Separation. *J. Inorg. Organomet. Polym.* **2023**, *33*, 1757–1781.

18. Lu, X.; Zhang, P.; Pan, H.; et al. Ionic Porous Materials: From Synthetic Strategies to Applications in Gas Separation and Catalysis. *Chem. Soc. Rev.* **2025**, *54*, 3061–3139.
19. Hwang, J.; Ejsmont, A.; Freund, R.; et al. Controlling the Morphology of Metal–Organic Frameworks and Porous Carbon Materials: Metal Oxides as Primary Architecture-Directing Agents. *Chem. Soc. Rev.* **2020**, *49*, 3348–3422.
20. Xu, S.; Dong, A.; Hu, Y.; et al. Multidimensional MOF-Derived Carbon Nanomaterials for Multifunctional Applications. *J. Mater. Chem. A* **2023**, *11*, 9721–9747.
21. Mansingh, S.; Subudhi, S.; Sultana, S.; et al. Cerium-Based Metal–Organic Framework Nanorods Nucleated on CeO_2 Nanosheets for Photocatalytic N_2 Fixation and Water Oxidation. *ACS Appl. Nano Mater.* **2021**, *4*, 9635–9652.
22. Wang, Y.; Ma, J.; Jin, F.; et al. Recent Advances in the Synthesis and Application of Monolayer 2D Metal-Organic Framework Nanosheets. *Small Sci.* **2024**, *4*, 2400132.
23. Chen, C.; Shen, L.; Wang, B.; et al. Environmental Applications of Metal–Organic Framework-Based Three-Dimensional Macrostructures: A Review. *Chem. Soc. Rev.* **2025**, *54*, 2208–2245.
24. Bhosale, R.; Gupta, S.; Kandasubramanian, B. Advances in Metal-Organic Frameworks for Use in 3D Printing Techniques. *ChemistrySelect* **2025**, *10*, e202404898.
25. Ndlwana, L.; Raleie, N.; Dimpe, K.M.; et al. Sustainable Hydrothermal and Solvothermal Synthesis of Advanced Carbon Materials in Multidimensional Applications: A Review. *Materials* **2021**, *14*, 5094.
26. Saleh, H.M.; Hassan, A.I. Synthesis and Characterization of Nanomaterials for Application in Cost-Effective Electrochemical Devices. *Sustainability* **2023**, *15*, 10891.
27. Jiang, Q.; Zhou, C.; Meng, H.; et al. Two-Dimensional Metal–Organic Framework Nanosheets: Synthetic Methodologies and Electrocatalytic Applications. *J. Mater. Chem. A* **2020**, *8*, 15271–15301.
28. Cao, W.; Liu, Y.; Xu, F.; et al. *In Situ* Electrochemical Synthesis of Rod-Like Ni-MOFs as Battery-Type Electrode for High Performance Hybrid Supercapacitor. *J. Electrochem. Soc.* **2019**, *167*, 050503.
29. Yang, Y.; Xu, D.; Lyu, L.; et al. Synthesis of MOF-Derived Fe_7S_8/C Rod-like Composites by Controlled Proportion of Carbon for Highly Efficient Electromagnetic Wave Absorption. *Compos. Part A Appl. Sci. Manuf.* **2021**, *142*, 106246.
30. Wu, Y.; Pang, H.; Yao, W.; et al. Synthesis of Rod-like Metal-Organic Framework (MOF-5) Nanomaterial for Efficient Removal of U(VI): Batch Experiments and Spectroscopy Study. *Sci. Bull.* **2018**, *63*, 831–839.
31. Sun, L.; Yin, M.; Li, Z.; et al. Facile Microwave-Assisted Solvothermal Synthesis of Rod-like Aluminum Terephthalate [MIL-53(Al)] for CO_2 Adsorption. *Ind. Eng. Chem. Res.* **2022**, *112*, 279–286.
32. Yang, H.; Zhao, Y.; Guo, Y.; et al. Surfactant-Mediated Crystalline Structure Evolution Enabling the Ultrafast Green Synthesis of Bismuth-MOF in Aqueous Condition. *Small* **2024**, *20*, 2307484.
33. Noa, F.M.A.; Abrahamsson, M.; Ahlberg, E.; et al. A Unified Topology Approach to Dot-, Rod-, and Sheet-MOFs. *Chem* **2021**, *7*, 2491–2512.
34. Li, R.-J.; Li, M.; Zhou, X.-P.; et al. A Highly Stable MOF with a Rod SBU and a Tetracarboxylate Linker: Unusual Topology and CO_2 Adsorption Behaviour under Ambient Conditions. *Chem. Commun.* **2014**, *50*, 4047–4049.
35. Won, S.; Jeong, S.; Kim, D.; et al. Transformation of a Cluster-Based Metal–Organic Framework to a Rod Metal–Organic Framework. *Chem. Mater.* **2022**, *34*, 273–278.
36. Li, R.-J.; Li, M.; Zhou, X.-P.; et al. ROD-8, a Rod MOF with a Pyrene-Cored Tetracarboxylate Linker: Framework Disorder, Derived Nets and Selective Gas Adsorption. *CrystEngComm* **2014**, *16*, 6291–6295.
37. Hoot, N.; Sheikhhosseini, E.; Ahmadi, S.A.; et al. Synthesis of Pyridone Derivatives Using 2D Rod like Bifunctional Fe Based MOF and CuO Nanocomposites as a Novel Heterogeneous Catalyst. *Sci. Rep.* **2023**, *13*, 15753.
38. Mukherjee, A.; Dhak, P.; Dhak, D. The Solvothermal Synthesis of a 3D Rod-like Fe–Al Bimetallic Metal–Organic-Framework for Efficient Fluoride Adsorption and Photodegradation of Water-Soluble Carcinogenic Dyes. *Environ. Sci. Adv.* **2022**, *1*, 121–137.
39. Xiao, Y.; Lin, Z.-H.; Li, M.; et al. Ultrafast Scale-up Synthesis of Calcium Rod/Layer MOFs and Luminescence Detection of Water in Organic Solvents. *Mater. Adv.* **2020**, *1*, 689–697.
40. Zhao, M.; Wang, Y.; Ma, Q.; et al. Ultrathin 2D Metal–Organic Framework Nanosheets. *Adv. Mater.* **2015**, *27*, 7372–7378.
41. Pham, M.-H.; Vuong, G.-T.; Fontaine, F.-G.; et al. Rational Synthesis of Metal–Organic Framework Nanocubes and Nanosheets Using Selective Modulators and Their Morphology-Dependent Gas-Sorption Properties. *Cryst. Growth Des.* **2012**, *12*, 3091–3095.
42. Xue, Y.; Zhao, G.; Yang, R.; et al. 2D Metal–Organic Framework-Based Materials for Electrocatalytic, Photocatalytic and Thermocatalytic Applications. *Nanoscale* **2021**, *13*, 3911–3936.
43. Liu, Y.-L.; Liu, X.-Y.; Feng, L.; et al. Two-Dimensional Metal–Organic Framework Nanosheets: Synthesis and Applications in Electrocatalysis and Photocatalysis. *ChemSusChem* **2022**, *15*, e202102603.
44. Huang, C.; Sun, W.; Jin, Y.; et al. A General Synthesis of Nanostructured Conductive Metal–Organic Frameworks from Insulating MOF Precursors for Supercapacitors and Chemiresistive Sensors. *Angew. Chem. Int. Ed.* **2024**, *63*, e202313591.
45. Xie, Y.; Wu, X.; Shi, Y.; et al. Recent Progress in 2D Metal-Organic Framework-Related Materials. *Small* **2024**, *20*, 2305548.

46. Wang, G.; Lu, J.; Fang, C.; et al. Ultrathin Metal–Organic Framework Nanosheets as Building Blocks of Lamellar Nanofilms for Ultrafast Molecular Sieving. *Nanoscale* **2022**, *14*, 17670–17680.
47. Doustkhah, E.; Hassandoost, R.; Khataee, A.; et al. Hard-Templated Metal–Organic Frameworks for Advanced Applications. *Chem. Soc. Rev.* **2021**, *50*, 2927–2953.
48. Huang, L.; Zhang, X.; Han, Y.; et al. *In Situ* Synthesis of Ultrathin Metal–Organic Framework Nanosheets: A New Method for 2D Metal-Based Nanoporous Carbon Electrocatalysts. *J. Mater. Chem. A* **2017**, *5*, 18610–18617.
49. Wang, L.; Saji, S.E.; Wu, L.; et al. Emerging Synthesis Strategies of 2D MOFs for Electrical Devices and Integrated Circuits. *Small* **2022**, *18*, 2201642.
50. Zacher, D.; Schmid, R.; Wöll, C.; et al. Surface Chemistry of Metal–Organic Frameworks at the Liquid–Solid Interface. *Angew. Chem. Int. Ed.* **2011**, *50*, 176–199.
51. Ohata, T.; Nomoto, A.; Watanabe, T.; et al. Air/Liquid Interfacial Formation Process of Conductive Metal–Organic Framework Nanosheets. *J. Colloid Interface Sci.* **2023**, *651*, 769–784.
52. Wang, M.; Dong, X.; Meng, Z.; et al. An Efficient Interfacial Synthesis of Two-Dimensional Metal–Organic Framework Nanosheets for Electrochemical Hydrogen Peroxide Production. *Angew. Chem. Int. Ed.* **2021**, *60*, 11190–11195.
53. Gumilar, G.; Valentino Kaneti, Y.; Henzie, J.; et al. General Synthesis of Hierarchical Sheet/Plate-like M-BDC (M = Cu, Mn, Ni, and Zr) Metal–Organic Frameworks for Electrochemical Non-Enzymatic Glucose Sensing. *Chem. Sci.* **2020**, *11*, 3644–3655.
54. Chang, Y.; Zhang, J.; Lu, R.; et al. Sheet-on-Sheet Architectural Assembly of MOF/Graphene for High-Stability NO Sensing at Room Temperature. *J. Mater. Chem. C* **2024**, *12*, 7520–7531.
55. Zhan, G.; Zeng, H.C. Synthesis and Functionalization of Oriented Metal–Organic-Framework Nanosheets: Toward a Series of 2D Catalysts. *Adv. Funct. Mater.* **2016**, *26*, 3268–3281.
56. Zhao, Y.; Wang, J.; Pei, R. Micron-Sized Ultrathin Metal–Organic Framework Sheet. *J. Am. Chem. Soc.* **2020**, *142*, 10331–10336.
57. Cao, X.; Zhang, L.; Chen, T.; et al. MOF Based Sheet-Assembled Flowers CdS-MoS_2 Composite for Enhanced Visible-Light Hydrogen Production. *Appl. Surf. Sci.* **2020**, *511*, 145355.
58. Li, F.-L.; Wang, P.; Huang, X.; et al. Large-Scale, Bottom-Up Synthesis of Binary Metal–Organic Framework Nanosheets for Efficient Water Oxidation. *Angew. Chem.* **2019**, *131*, 7125–7130.
59. Liu, Y.; He, X.; Wang, Y.; et al. Controlled Synthesis of MOF-Derived Nano–Microstructure toward Lightweight and Wideband Microwave Absorption. *Small* **2023**, *19*, 2302633.
60. Qu, Y.; Shi, C.; Cao, H.; et al. Synthesis of Ni-MOF/$Ti_3C_2T_x$ Hybrid Nanosheets via Ultrasonific Method for Supercapacitor Electrodes. *Mater. Lett.* **2020**, *280*, 128526.
61. Wang, Z.; Zhu, J.; Xu, S.; et al. Graphene-like MOF Nanosheets Stabilize Graphene Oxide Membranes Enabling Selective Molecular Sieving. *J. Membr. Sci.* **2021**, *633*, 119397.
62. Phan, P.T.; Hong, J.; Tran, N.; et al. The Properties of Microwave-Assisted Synthesis of Metal–Organic Frameworks and Their Applications. *Nanomaterials* **2023**, *13*, 352.
63. Zhu, Y.-J.; Chen, F. Microwave-Assisted Preparation of Inorganic Nanostructures in Liquid Phase. *Chem. Rev.* **2014**, *114*, 6462–6555.
64. Mishra, R.K.; Yadav, A.; Mishra, V.; et al. Fundamental Theory of Electromagnetic Spectrum, Dielectric and Magnetic Properties, Molecular Rotation, and the Green Chemistry of Microwave Heating Equipment. In *Green Chemical Synthesis with Microwaves and Ultrasound*; John Wiley & Sons: Hoboken, NJ, USA, 2024; pp. 21–67.
65. Babu, R.; Roshan, R.; Kathalikkattil, A.C.; et al. Rapid, Microwave-Assisted Synthesis of Cubic, Three-Dimensional, Highly Porous MOF-205 for Room Temperature CO_2 Fixation via Cyclic Carbonate Synthesis. *ACS Appl. Mater. Interfaces* **2016**, *8*, 33723–33731.
66. Ataei, F.; Dorranian, D.; Motakef-Kazemi, N. Synthesis of MOF-5 Nanostructures by Laser Ablation Method in Liquid and Evaluation of Its Properties. *J. Mater. Sci. Mater. Electron.* **2021**, *32*, 3819–3833.
67. Greer, H.F.; Liu, Y.; Greenaway, A.; et al. Synthesis and Formation Mechanism of Textured MOF-5. *Cryst. Growth Des.* **2016**, *16*, 2104–2111.
68. Fazio, E.; Gökce, B.; Giacomo, A.D.; et al. Nanoparticles Engineering by Pulsed Laser Ablation in Liquids: Concepts and Applications. *Nanomaterials* **2020**, *10*, 2317.
69. Kim, J.H.; Choi, H.W. Review on Principal and Applications of Temporal and Spatial Beam Shaping for Ultrafast Pulsed Laser. *Photonics* **2024**, *11*, 1140.
70. Varsha, M.V.; Nageswaran, G. Review—Direct Electrochemical Synthesis of Metal Organic Frameworks. *J. Electrochem. Soc.* **2020**, *167*, 155527.
71. Xiao, X.; Zou, L.; Pang, H.; et al. Synthesis of Micro/Nanoscaled Metal–Organic Frameworks and Their Direct Electrochemical Applications. *Chem. Soc. Rev.* **2020**, *49*, 301–331.

72. Yang, H.M.; Song, X.L.; Yang, T.L.; et al. Electrochemical Synthesis of Flower Shaped Morphology MOFs in an Ionic Liquid System and Their Electrocatalytic Application to the Hydrogen Evolution Reaction. *RSC Adv.* **2014**, *4*, 15720–15726.
73. Bang, J.H.; Suslick, K.S. Applications of Ultrasound to the Synthesis of Nanostructured Materials. *Adv. Mater.* **2010**, *22*, 1039–1059.
74. Safarifard, V.; Morsali, A. Facile Preparation of Nanocubes Zinc-Based Metal-Organic Framework by an Ultrasound-Assisted Synthesis Method; Precursor for the Fabrication of Zinc Oxide Octahedral Nanostructures. *Ultrason. Sonochem.* **2018**, *40*, 921–928.
75. Guo, Z.; Zhao, X.; Chen, G.; et al. Controllable Synthesis of Magic Cube-like Ce-MOF-Derived Pt/CeO_2 Catalysts for Formaldehyde Oxidation. *Nanoscale* **2022**, *14*, 12713–12721.
76. Kimitsuka, Y.; Hosono, E.; Ueno, S.; et al. Fabrication of Porous Cubic Architecture of ZnO Using Zn-Terephthalate MOFs with Characteristic Microstructures. *Inorg. Chem.* **2013**, *52*, 14028–14033.
77. Lammert, M.; Glißmann, C.; Reinsch, H.; et al. Synthesis and Characterization of New Ce(IV)-MOFs Exhibiting Various Framework Topologies. *Cryst. Growth Des.* **2017**, *17*, 1125–1131.
78. Das, M.C.; Xu, H.; Xiang, S.; et al. A New Approach to Construct a Doubly Interpenetrated Microporous Metal–Organic Framework of Primitive Cubic Net for Highly Selective Sorption of Small Hydrocarbon Molecules. *Chem. Eur. J.* **2011**, *17*, 7817–7822.
79. Koolivand, M.; Nikoorazm, M.; Ghorbani-Choghamarani, A.; et al. A Novel Cubic Zn-Citric Acid-Based MOF as a Highly Efficient and Reusable Catalyst for the Synthesis of Pyranopyrazoles and 5-Substituted 1H-Tetrazoles. *Appl. Organomet. Chem.* **2022**, *36*, e6656.
80. Zhang, C.; Wang, P.; Li, W.; et al. MOF-Assisted Synthesis of Octahedral Carbon-Supported PtCu Nanoalloy Catalysts for an Efficient Hydrogen Evolution Reaction. *J. Mater. Chem. A* **2020**, *8*, 19348–19356.
81. Reinsch, H. "Green" Synthesis of Metal-Organic Frameworks. *Eur. J. Inorg. Chem.* **2016**, *2016*, 4290–4299.
82. Dai, S.; Nouar, F.; Zhang, S.; et al. One-Step Room-Temperature Synthesis of Metal(IV) Carboxylate Metal—Organic Frameworks. *Angew. Chem.* **2021**, *133*, 4328–4334.
83. Zou, F.; Hu, X.; Li, Z.; et al. MOF-Derived Porous ZnO/$ZnFe_2O_4$/C Octahedra with Hollow Interiors for High-Rate Lithium-Ion Batteries. *Adv. Mater.* **2014**, *26*, 6622–6628.
84. Wu, R.; Qian, X.; Yu, F.; et al. MOF-Templated Formation of Porous CuO Hollow Octahedra for Lithium-Ion Battery Anode Materials. *J. Mater. Chem. A* **2013**, *1*, 11126–11129.
85. Minh, T.T.; Tu, N.T.T.; Van Thi, T.T.; et al. Synthesis of Porous Octahedral ZnO/CuO Composites from Zn/Cu-Based MOF-199 and Their Applications in Visible-Light-Driven Photocatalytic Degradation of Dyes. *J. Nanomater.* **2019**, *2019*, 5198045.
86. Song, M.; Song, X.; Liu, X.; et al. Enhancing Photocatalytic CO_2 Reduction Activity of $ZnIn_2S_4$/MOF-808 Microsphere with S-Scheme Heterojunction by *in Situ* Synthesis Method. *Chin. J. Catal.* **2023**, *51*, 180–192.
87. Yang, Y.; Dong, H.; Wang, Y.; et al. Synthesis of Octahedral like Cu-BTC Derivatives Derived from MOF Calcined under Different Atmosphere for Application in CO Oxidation. *J. Solid State Chem.* **2018**, *258*, 582–587.
88. Chimupala, Y.; Kaeosamut, N.; Yimklan, S. Octahedral to Tetrahedral Conversion upon a Ligand-Substitution-Induced Single-Crystal to Single-Crystal Transformation in a Rectangular Zn(II) Metal–Organic Framework and Its Photocatalysis. *Cryst. Growth Des.* **2021**, *21*, 5373–5382.
89. Hu, S.; Liu, M.; Li, K.; et al. Solvothermal Synthesis of NH_2-MIL-125(Ti) from Circular Plate to Octahedron. *CrystEngComm* **2014**, *16*, 9645–9650.
90. Shi, W.; Li, T.; Chu, N.; et al. Nano-Octahedral Bimetallic Fe/Eu-MOF Preparation and Dual Model Sensing of Serum Alkaline Phosphatase (ALP) Based on Its Peroxidase-like Property and Fluorescence. *Mater. Sci. Eng. C* **2021**, *129*, 112404.
91. Zhao, P.; Qin, F.; Huang, Z.; et al. MOF-Derived Hollow Porous Ni/CeO_2 Octahedron with High Efficiency for N_2O Decomposition. *Chem. Eng. J.* **2018**, *349*, 72–81.
92. Wu, R.; Wang, D.P.; Kumar, V.; et al. MOFs-Derived Copper Sulfides Embedded within Porous Carbon Octahedra for Electrochemical Capacitor Applications. *Chem. Commun.* **2015**, *51*, 3109–3112.
93. Nangia, A.K.; Desiraju, G.R. Crystal Engineering: An Outlook for the Future. *Angew. Chem. Int. Ed.* **2019**, *58*, 4100–4107.
94. Raganati, F.; Miccio, F.; Ammendola, P. Adsorption of Carbon Dioxide for Post-Combustion Capture: A Review. *Energy Fuels* **2021**, *35*, 12845–12868.
95. Li, B.; Ma, J.-G.; Cheng, P. Integration of Metal Nanoparticles into Metal–Organic Frameworks for Composite Catalysts: Design and Synthetic Strategy. *Small* **2019**, *15*, 1804849.
96. Ha, J.; Hwa Lee, J.; Ri Moon, H. Alterations to Secondary Building Units of Metal–Organic Frameworks for the Development of New Functions. *Inorg. Chem. Front.* **2020**, *7*, 12–27.
97. Zhu, H.; Liu, D. The Synthetic Strategies of Metal–Organic Framework Membranes, Films and 2D MOFs and Their Applications in Devices. *J. Mater. Chem. A* **2019**, *7*, 21004–21035.
98. Xu, D.; Ding, Q.; Li, J.; et al. A Sheet-like MOF-Derived Phosphorus-Doped Porous Carbons for Supercapacitor Electrode Materials. *Inorg. Chem. Commun.* **2020**, *119*, 108141.

99. Peng, Y.; Sanati, S.; Morsali, A.; et al. Metal–Organic Frameworks as Electrocatalysts. *Angew. Chem. Int. Ed.* **2023**, *62*, e202214707.
100. Lu, Z.; Luo, W.; Huang, X.; et al. Highly-Stable Cobalt Metal Organic Framework with Sheet-like Structure for Ultra-Efficient Water Oxidation at High Current Density. *J. Colloid Interface Sci.* **2022**, *611*, 599–608.
101. Kudapa, V.K.; Paliyal, P.S.; Mondal, A.; et al. A Critical Review of Fabrication Strategies, Separation Techniques, Challenges, and Future Prospects for the Hydrogen Separation Membrane. *Fusion Sci. Technol.* **2024**, *80*, 803–825.